

Research Article

Mechanical Properties of High-Tech Fiber Bundles Reinforced Composites by 3D Printing

Wang YY, Jiang HY, Tuo XH*, Gong YM and Guo J

School of Textile and Material Engineering, Dalian Polytechnic University, China

*Corresponding author: Xiao Hang Tuo, School of Textile and Material Engineering, Dalian Polytechnic University, Dalian, 116034, China

Received: April 28, 2020; Accepted: May 18, 2020;

Published: May 25, 2020

Abstract

Rule of Mixtures (RoMs) is a theoretical hypothesis that describes the mechanical properties of the fiber-reinforced composites. RoMs provides the relevant parameters based on the complexity of the reinforcing materials. However, even if the continuous unidirectional fiber is used as a reinforcing material, its mechanical performance in the composite is also limited.

In this paper, the reliability of RoMs was evaluated and the verifiable sample was designed with the 3D printing technology. The difference between the actual measured value and the theoretical prediction value was compared, and the factors influencing the reliability of RoMs were analyzed. Based on the results, the strength of the fiber bundles in the composite materials had decreased significantly. The fiber had only enhanced the axial force of fiber-reinforced composites while the Poisson's ratio of the components in the composite had not been consistent. These influencing factors could provide some references for understanding the mechanical mechanism of the fiber-reinforced composites, bringing the enhancement effect and perfecting the theoretical hypothesis.

Keywords: High-tech fiber; 3D printing; Rule of mixtures; Mechanical property

Introduction

The theoretical study of the fiber-reinforced composites is based on the Rule of Mixtures (RoMs) that has gradually developed. The fiber, as a reinforcing material, can be classified as continuous and discontinuous or simply known as long and short fibers [1]. Cox [2] proposed a shear-lag model to calculate the modulus of the discontinuous unidirectional fiber composites. But the short fiber, it has no capacity to continuously bear the external force for the matrix material. Also, there are complexities seen in the fiber orientation and length. Thus, Krenche [3] suggested the concept of fiber orientation and created a model. Kelly and Tyson [4] also proposed using the critical fiber length to identify its effect. However, both models, developed by Krenche and Kelly-Tyson, only provided a theoretical process for estimating RoMs. To improve the RoMs practicability, Halpin and Tsai [5] tried to predict the mechanical properties of the composites using a similar empirical method. Currently, the modified RoMs by Futian, Kawada [6], and Zhou [7] has been widely recognized but the development of the theoretical formula has not met the expectations of its practical application, and thus, the more complex theoretical formulas have been proposed [8,9].

In the practical application, the study on the long-fiber-reinforced composites is focused on the carbon fiber reinforced epoxy resin because the arrangement of continuous unidirectional fiber is very regular, satisfying the ideal mechanical prediction model. Kim et al., analyzed the carbon material reinforced epoxy resin composite material by using vacuum molding technology [10]. The study of the short fiber-reinforced composites is relatively difficult, mainly because of the fiber length and the irregular distribution in the matrix. Bast fibers have the advantages of high specific strength, environmental protection, and high efficiency of the surface treatment, and are

oftentimes studied as short fiber reinforcements. Ku et al., evaluated the RoMs reliability for natural fiber-reinforced composites [11]. Regarding the selection of the matrix material, thermosetting resin has been seen with high fluidity and can be better contacted with reinforcing material to improve the stability of the composites. The commonly used thermoplastic materials have better thermal and mechanical properties but their high viscosity can damage the order arrangement of fibers, making them unsuitable for the matrix material of long-fiber-reinforced composites. Through the application of linear 3D printing technology [12], the thermoplastic material can be integrated as a matrix part of the hollow shaped composite material [13]. The fibers can be arranged in an order state in this structure [14]. Hinchcliffe et al., validated the theoretical prediction of the jute and flax-reinforced hollow 3D printing materials using the experimental methods [15]. Recently, the continuous carbon fiber-reinforced 3D printing supplies and products have been developed [16-18]. Jahangir et al., [19] studied a 3D printed continuous carbon fiber reinforced polycarbonate composite. It was confirmed that the carbon fiber content and the combined effect with the matrix had a great influence on the composite properties.

In this paper, the verifiable tensile sample of the continuous fiber-reinforced composites was designed using the 3D printing technique with emphasis on the theoretical formula of fiber-reinforced composites [20]. Among them, the common 3D printing materials, such as PLA [21], ABS [22], and HIPS filaments, are compared as matrix materials [23]. The high-tech fibers were selected as reinforcing fibers, along with carbon fiber [24], basalt fiber [25], ultra-high molecular weight fiber polyethylene [26] and aramid fiber [27], which have excellent performance and stable structure. The four fiber materials were treated with an adhesive used in the fiber rod

and filled into the hollow 3D printing matrix. The predicted values and the measured values were compared to verify the reliability of the theoretical hypothesis and use as a new baseline or valuable practical reference for the theory development.

Material and Methods

Materials

The four high-tech fibers selected in this paper were ultra-high molecular weight Polyethylene Fiber ([PF], TFXC 400-C, Shandong Taifeng Mining Co., Ltd. China), Basalt Fiber ([BF], Roving, Haining Anjie Composite Materials Co., Ltd. China), Carbon Fiber ([CF], HTA-W1K, Toho Co., Ltd. Japan), and Aromatic polyamide Fiber ([AF], Twaron 2200, Diren Co., Ltd. Japan). A number of roots in each fiber bundle were 400, 600, 1000, and 400, respectively. The diameters of each fiber were 20 μ m, 12 μ m, 7 μ m, and 8 μ m, respectively. Based on the given data, the cross-sectional area of each fiber bundle could be easily calculated, which was prepared to identify the tensile strength of the fiber bundle.

The linear 3D printing supplies were PLA, ABS and HIPS (diameter 1.73mm, Shenzhen 3DSWAY Technology Co., Ltd), which were the main composite matrix materials. Silicone (601, Beijing Haibei Si Company) was used as a mold material for stretching the samples. Adhesive (PSK12CT, Shanghai Henkel Co., Ltd) was selected to bond the fibers and matrix materials.

Preparation and testing of reinforcing materials

An adhesive was used to bond the four fiber materials into fiber rods with a radius of 1mm. As used in Figure 1 and among others, the root numbers of the filling fiber (bundle \times root) were PE (16 \times 400); BF (2 \times 600); CF (3 \times 1000), and AF (2 \times 400).

The method of stretching the fiber bundle (ASTM D 3822-01) was referred. The tensile test was held at both of the fiber rods' ends Figure 2. The tensile speed was 5mm/min while the fixture distance was 110mm, which was consistent with the condition of dumbbell tensile sample. Meanwhile, the yarn strength of the four fiber bundles having 100mm in length each was also tested and compared with the strength of the fiber rods [28,29].

3D printing matrix materials

Using the standard size (GB/T1040) of the test sample, the shape design and molding conditions of the matrix materials were set with the 3D tooling software (Pro/engineer 5.0 and Cura 15.02.1) and the 3D printer (Z-603S high-precision 3D printer, Shenzhen Aurora Technology Co., Ltd). To better compare the fiber reinforcement results, the four sets of 3D printing matrix models were designed Figure 3, namely: no tunnel, single tunnel, double tunnel, and triple tunnel with the tunneling radius of 1mm as the length of the sample. The three kinds of 3D matrix materials were PLA, ABS, and HIPS (diameter 1.73mm, Shenzhen 3DSWAY Technology Co., Ltd.). The nozzle and heating table temperatures of PLA were 215 $^{\circ}$ C and 50 $^{\circ}$ C while ABS and HIPS were 240 $^{\circ}$ C and 100 $^{\circ}$ C, respectively. The print speed was 40mm/s and 100% filled.

Preparation and testing of composites

The four high-tech fiber rods were inserted and fixed into the tunnel of tensile samples. The sample fiber-reinforced PLA composite was shown in Figure 4. The bending samples were also created with the

same process, such as in Figure 5, with the matrix ABS as an example. The mechanical testing conditions of the fiber-reinforced composites were tensile speed (5mm/min), fixture distance (110mm), bending speed (2mm/min), and the distance between fulcrums (36mm).

The formulas for calculating the tensile strength (Equation 1) and the bending strength (Equation 2) are as follows:

$$\sigma = \frac{F}{A} \quad (1)$$

$$R = \frac{3PL}{2bh^2} \quad (2)$$

where σ , F and A are for tensile strength, tensile force and cross-sectional area of the tensile samples, respectively. R, P, L, b and h represent the bending strength, maximum force and distance between fulcrums, height and width of the bending samples.

Equation 3 is the modified Rule of Mixtures (mRoMs) for predicting the tensile strength of the composites [30,31]. Since the reinforcing fibers are continuous and the orientation is along the stretching axis, the fiber parameters can be ignored and may not be indicated.

$$\sigma_c = \sigma_f V_f + \sigma_m V_m \quad (3)$$

σ_c , σ_f and σ_m are the tensile strengths of the composite, reinforcement, and matrix. V_f and V_m are the volume ratios of the reinforcement and matrix.

Results and Discussion

Tensile strength of fiber bundles and fiber rods

The fiber rod, as a reinforcement of the composite material, had reduced strength compared to the uncured fiber bundle, with the strength ratio of about 1:10 Figure 5. The adhesive brought some internal stress in the fiber rod to undermine the structural characteristics of fibers to a certain extent. These internal stresses caused the shearing force to increase when the composite material was stretched. Therefore, this finding showed that when predicting the mechanical properties of the composite, the strength value of fiber could not be directly used as a reinforcement parameter. The value of reinforcement parameter was also linked between the fibers, and the interface force between the fiber and matrix.

Mechanical properties of fiber-reinforced composites

The effects of the four high-tech fibers in enhancing the mechanical properties of the three 3D printing matrix materials were different. Initially, as cited, the three matrix materials, based on the order of PLA, ABS, and HIPS, their rigidity were gradually weakened while their flexibility became strong. So the tensile strength of the fiber-reinforced composites was gradually stronger, as shown in Figure 6&8a. Among them, the reinforcing effect of PE on HIPS was the best, the effect of CF was the best on ABS, the effect of AF was the best on PLA, and the reinforcing effect of BF is the least compared to the other fibers.

For the flexural strength of the fiber-reinforced composite, the reinforcing effect of fibers was not obvious as shown in Figure 7&8b. From the data part, when the fiber content was increased, the bending strength of composite material decreased. Although the fine fibers could be used, enabling the fiber bundles to bend easily, the four high-tech fibers had become brittle after being treated by the adhesive,

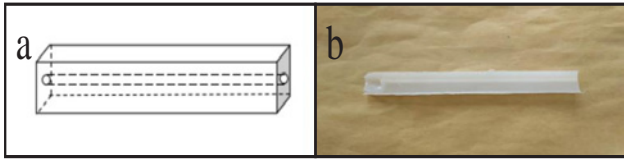


Figure 1: Design model (a) and entity diagram (b) of silicone mold.

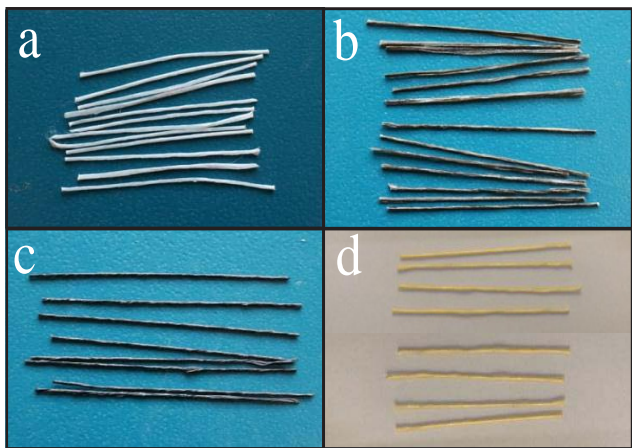


Figure 2: Four high-tech fiber rods: (a) PE (UHMWPE fiber); (b) BF (basalt fiber); (c) CF (carbon fiber); (d) AF (aramid fiber).

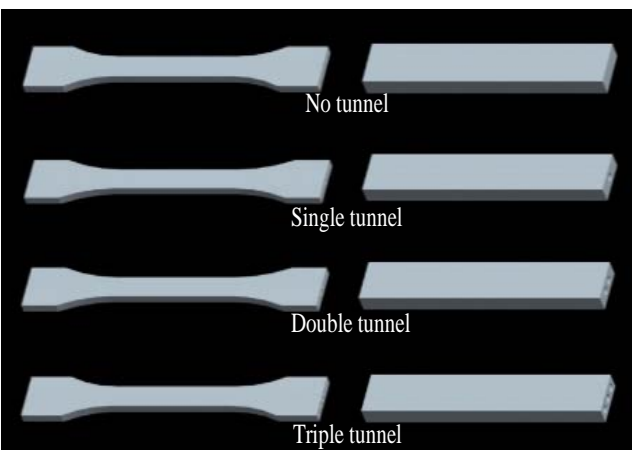


Figure 3: Four sets of 3D printing matrix models (for tensile and bending tests).

which was clearly shown in the bending results.

Verification analysis of RoMs

Figure 9,10,11 showed the graphs comparing the actual measured values of the tensile strength of fiber-reinforced composite and the calculated values using RoMs. From the enhancement effects of the three different 3D printing matrix materials, the actual measured value and the predicted calculated value were substantially the same in terms of the low component. This validated the RoMs theory and indirectly showing that it was possible to provide an ideal verification sample similar to the theoretical hypothesis by 3D printing. However, in the case of high composition, the difference between actual

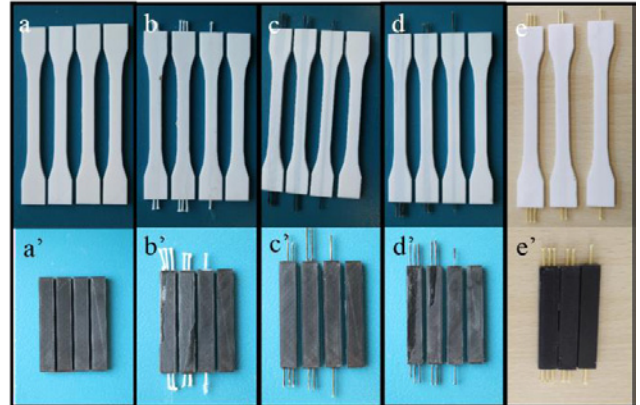


Figure 4: Four fiber reinforced 3D printing materials (PLA tensile samples and ABS bending samples).

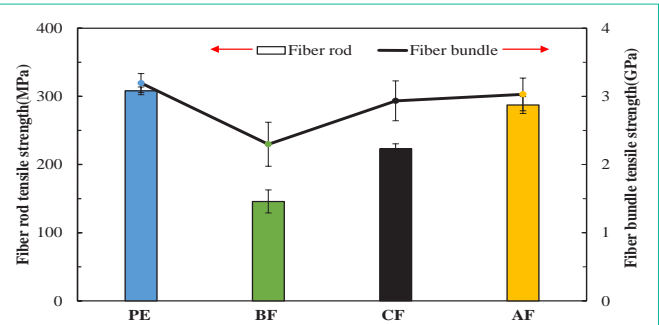


Figure 5: Tensile strength of four high-tech fiber bundles and their fiber rods.

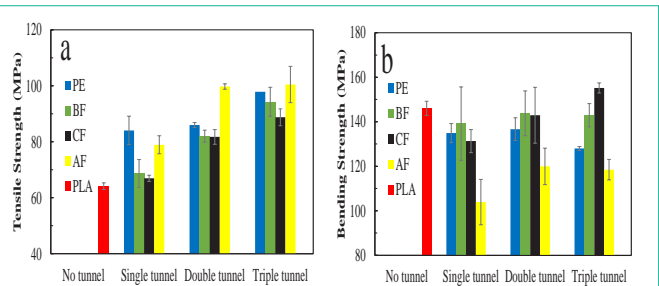


Figure 6: Tensile strength and bending strength of PLA and its multi-tunnel composite.

measured value and predicted calculated value was huge, especially in PE and AF, where the actual measured value was initially less than the prediction calculation value. This was because PE and AF were different from BF and CF, as they would be through the deformation to weaken a part of the tensile force. The RoMs formula was based on the assumption that the Poisson's ratio of the reinforcing material and the matrix material was equal. For BF and CF, as inorganic materials, their Poisson's ratio was much smaller than the organic materials such as PE and AF. In the tensile deformation in the matrix material, the smallest was PLA while the largest was HIPS. Therefore, the major reason that the calculated values could not be well predicted for the actual measurements was that the deformation of each component in composite was inconsistent. The result in the composite material was being subjected to the external stretching, while the resistance

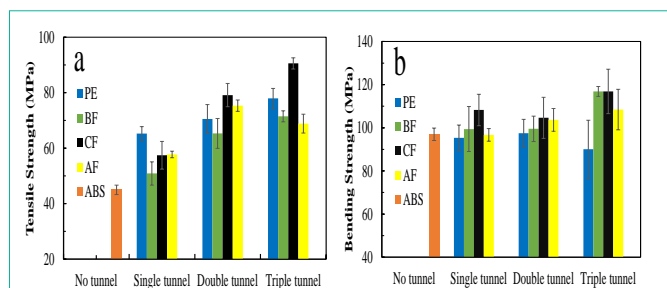


Figure 7: Tensile strength and bending strength of ABS and its multi-tunnel composite.

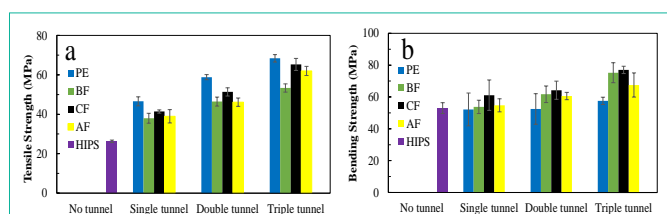


Figure 8: Tensile strength and bending strength of HIPS and its multi-tunnel composite.

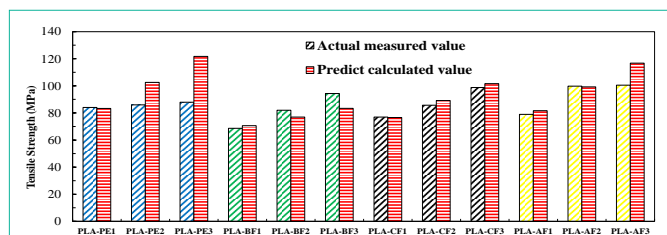


Figure 9: Verification of tensile strength of high-tech fiber reinforced PLA composite.

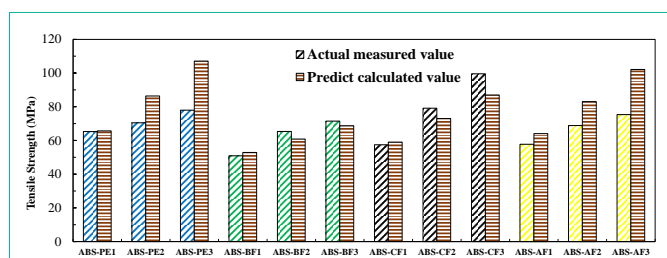


Figure 10: Verification of tensile strength of high-tech fiber reinforced ABS composite.

of each component was not the same and synchronized. Thus, this had caused the overall mechanical performance of the composite materials to be restricted.

Conclusions

In this study, 3D printing technique was used to create the verifiable samples consistent with the RoMs theory. In preparing the reinforcing material, the strength of fiber rod was tested to be significantly smaller than the fiber bundle strength. Therefore, the data information of reinforcing materials needed should be measured using the actual measurement. Through the mechanical measurement of the composite, the reinforcing fibers had shown a certain effect on the tensile strength of matrix. This effect was increased with more

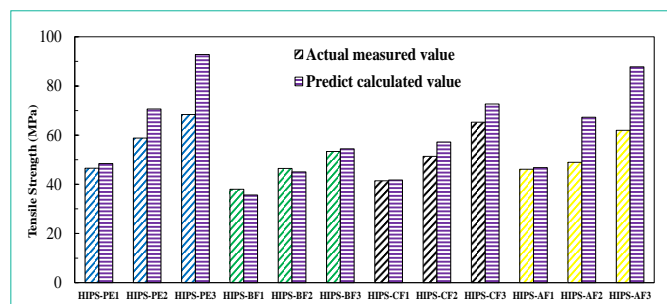


Figure 11: Verification of tensile strength of high-tech fiber reinforced HIPS composite.

fiber content. However, the reinforcing fibers had no significant enhancement effect on the flexural strength of the composites and even had a reduced adverse effect. The reason was that after the fiber bundle was treated with adhesives, the brittleness of fiber rod became larger, especially when in perpendicular to the fiber axis direction, and the high flexibility of fiber material also reduced the bending strength of composite materials.

The parameters of each component were included in the RoMs formula, calculated and compared the measured values of the fiber-reinforced composites. Through the experimental design method of this paper, the RoMs reliability was verified, presenting the limitations of RoMs.

Acknowledgement

This work was supported by Science and Technology Plan Project of Liaoning Province, China (2019-ZD-0284) and Deyang Zhao (United Creation Packaging Solutions Sheng Dao (DaLian) Co., Ltd).

References

- Hyer MW, Waas AM. Micromechanics of linear elastic continuous fiber composites. 2000.
- Cox HL. The elasticity and strength of paper and other fibrous materials. Br J Appl Phys. 1952; 3: 72.
- Krenchel H. Fibre reinforcement; theoretical and practical investigations of the elasticity and strength of fibre-reinforced materials. 1964.
- Kelly A, Tyson AW. Tensile properties of fibre-reinforced metals: copper/tungsten and copper/molybdenum. J Mech Phys Solids. 1965; 13: 329-350.
- Halpin JC. Effects of environmental factors on composite materials (No. AFML-TR-67-423). Air Force Materials Lab Wright-Patterson AFB OH. 1969.
- Fukuda H, Kawata K. On Young's modulus of short fibre composites. Fibre Sci. Technol. 1974; 7: 207-222.
- Fukuda H, Chou TW. A Probabilistic Theory of the Strength of Short-Fibre Composites with Variable Fibre Length and Orientation. J Mater Sci. 1982; 17: 1003-1011.
- Faruk O, Bledzki AK, Fink HP, Sain M. Biocomposites reinforced with natural fibers: 2000-2010. Prog. Polym. Sci. 2012; 37: 1552-1596.
- Hine P, Parveen B, Brands D, Caton-Rose F. Validation of the modified rule of mixtures using a combination of fibre orientation and fibre length measurements. Composites Part A. 2014; 64: 70-78.
- Kim H, Oh E, Hahn HT, Lee KH. Enhancement of fracture toughness of hierarchical carbon fiber composites via improved adhesion between carbon nanotubes and carbon fibers. Composites Part A. 2015; 71: 72-83.
- Ku H, Wang H, Pattarachaiyakop N, Trada M. A review on the tensile properties of natural fiber reinforced polymer composites. Composites Part B. 2011; 2: 856-873.

12. Wang X, Jiang M, Zhou Z, Gou J, Hui D. 3D printing of polymer matrix composites: A review and prospective. *Composites Part B*. 2017; 110: 442-458.
13. Roberson D, Shemelya CM, MacDonald E, Wicker R. Expanding the applicability of FDM-type technologies through materials development. *Rapid Prototyping Journal*. 2015.
14. Tian X, Liu T, Wang Q, Dilmurat A, Li D, Ziegmann G. Recycling and remanufacturing of 3D printed continuous carbon fiber reinforced PLA composites. *J Cleaner Prod*. 2017; 142: 1609-1618.
15. Hinchcliffe SA, Hess KM, Srubar III WV. Experimental and theoretical investigation of prestressed natural fiber-reinforced Poly(lactic acid) (PLA) composite materials. *Composites Part B*. 2016; 95: 346-354.
16. Ning F, Cong W, Hu Y, Wang H. Additive manufacturing of carbon fiber-reinforced plastic composites using fused deposition modeling: Effects of process parameters on tensile properties. *J Compos Mater*. 2017; 51: 451-462.
17. Li N, Li Y, Liu S. Rapid prototyping of continuous carbon fiber reinforced poly(lactic acid) composites by 3D printing. *J Mater Process Technol*. 2016; 238: 218-225.
18. Hu C, Sun Z, Xiao Y, Qin Q. Recent patents in additive manufacturing of continuous fiber reinforced composites. *Recent Pat Mech Eng*. 2019; 12: 25-36.
19. Jahangir MN, Billah KMM, Lin Y, Roberson DA, Wicker RB, Espalin D. Reinforcement of material extrusion 3D printed polycarbonate using continuous carbon fiber. *Addit Manuf*. 2019; 28: 354-364.
20. Tuo X, Yu Y, Zhao Y, Gong Y, Guo J. Validation study on the theory of composites by using three-dimensional printing technology. *J Reinf Plast Compos*. 2018; 37: 1004-1010.
21. Afrose M, Masood SH, Iovenitti P, Nikzad M, Sbarski IF. Effects of part build orientations on fatigue behaviour of FDM-processed PLA material. *Progress in Additive Manufacturing*. 2016; 1: 21-28.
22. Türk DA, Brenni F, Zogg M, Meboldt M. Mechanical characterization of 3D printed polymers for fiber reinforced polymers processing. *Mater Des*. 2017; 118: 256-265.
23. Choi G, Kim S. Adaptive modeling method for 3-D printing with various polymer materials. *Fibers Polym*. 2016; 17: 977-983.
24. Brooks H, Molony S. Design and evaluation of additively manufactured parts with three dimensional continuous fibre reinforcement. *Mater Des*. 2016; 90: 276-283.
25. Dhand V, Mittal G, Rhee KY, Park SJ, Hui D. A short review on basalt fiber reinforced polymer composites. *Composites Part B*. 2015; 73: 166-180.
26. Huang W, Wang Y, Xia Y. Statistical dynamic tensile strength of UHMWPE-fibers. *Polymer*. 2004; 45: 3729-3734.
27. Bettini P, Alitta G, Sala G, Di Landro L. Fused deposition technique for continuous fiber reinforced thermoplastic. *J Mater Eng Perform*. 2017; 26: 843-848.
28. Ma Y, Yang Y, Sugahara T, Hamada H. A study on the failure behavior and mechanical properties of unidirectional fiber reinforced thermosetting and thermoplastic composites. *Composites Part B*. 2016; 99: 162-172.
29. Song J, Wen W, Cui H, Zhao S. Study on static and fatigue behaviors of carbon fiber bundle and the statistical distribution by experiments. *J Compos Mater*. 2015; 49: 3157-3168.
30. Espinach FX, Granda LA, Tarrés Q, Duran J, Fullana-i-Palmer P, Mutjé P. Mechanical and micromechanical tensile strength of eucalyptus bleached fibers reinforced polyoxymethylene composites. *Composites Part B*. 2017; 116: 333-339.
31. Khanlou HM, Woodfield P, Summerscales J, Francucci G, King B, Talebian S, et al. Estimation of mechanical property degradation of poly (lactic acid) and flax fibre reinforced poly (lactic acid) bio-composites during thermal processing. *Meas*. 2018; 116: 367-372.